

Improved electrochemical performance of Li-doped natural graphite anode for lithium secondary batteries

Young Tae Lee^a, Chong Seung Yoon^b, Yang-Kook Sun^{a,*}

^a Department of Chemical Engineering, Center for Information and Communication Materials, Hanyang University, 17 Haendang-Dong, Sunfdong-Gu, Seoul 133-791, South Korea

^b Division of Material Science and Engineering, Center for Information and Communication Materials, Hanyang University, 17 Haendang-Dong, Sunfdong-Gu, Seoul 133-791, South Korea

Received 19 April 2004; accepted 18 June 2004

Available online 11 September 2004

Abstract

Lithium-doped natural graphite is synthesized by a simple wet ball-milling method and use as an anode material in lithium secondary batteries. The modified natural graphite is examined with a view to improved cycleability and columbic efficiency on the first charge–discharge cycle (irreversible capacity loss). Lithium-doping results in marked improvements in electrochemical performance. These are investigated by means of X-ray powder diffraction, impedance measurement, high resolution transmission electron microscopy, field emission scanning electron microscopy, and measurement of electrochemical capacity. LiO_x intercalated at the edge planes reduces the electrolyte breakdown by passivating the highly reactive sites along these planes. The Li-doped natural graphite exhibits $\sim 5\%$ reduction in the first irreversible capacity while the reversible capacity remains unchanged in comparison with pristine graphite electrode. Also, it has an excellent capacity retention of $\sim 99\%$ after 50 cycles.

© 2004 Elsevier B.V. All rights reserved.

Keywords: Natural graphite; Lithium secondary batteries; Lithium-doping; LiO_x ; Solid electrolyte interface; Capacity

1. Introduction

Graphitic materials have been widely used as anode materials for lithium secondary batteries. Nevertheless, graphitic anodes still suffer from serious problems, that include electrolyte decomposition and subsequent surface film formation. These cause irreversible capacity changes during cycling [1,2], which give rise to detrimental effects such as high internal pressure and lower cycling efficiency. The irreversible reaction also deteriorates both the cathode material and the electrolyte [3,4]. Present commercial carbon materials, such as MCMB (mesocarbon microbeads) and MCF (mesocarbon fibre), have relatively higher cost and lower discharge capacity. Several materials, such as Sn-based ox-

ides [5–7] and graphite–Fe–Si–Sn alloy composites [8–10] have recently been reported as possible alternatives. Despite the huge theoretical capacity (maximum capacity of up to 4000 mAh g^{-1}) of these materials, a large capacity loss is the main limitation to their use as an anode material for the lithium secondary batteries.

Natural graphite is considered as another promising anode material for lithium secondary batteries because of its high reversible capacity, appropriate potential profile, and low cost. Nevertheless, a large irreversible capacity loss during the first cycle, poor cycleability and poor rate capability have prevented its practical use. Many research groups have reported, however, that surface pretreatment of natural graphite by mild oxidation [11,12], carbon coating [13,14] or polyelectrolyte adsorption [15] is effective in improving cycling efficiencies and reversible capacities.

In this study, it is shown that Li-doping treatment of natural graphite can greatly enhance long-term cycling perfor-

* Corresponding author. Tel.: +82 2 2290 0524; fax: +82 2 2282 7329.
E-mail address: yksun@hanyang.ac.kr (Y.-K. Sun).

mance. An attempt is made to reveal the structural changes responsible for this behaviour.

2. Experimental

Li-doped natural graphite was synthesized by a wet ball-milling method. The natural graphite (China) was mixed with lithium acetate ($\text{CH}_3\text{COOLi}\cdot 2\text{H}_2\text{O}$) in a weight ratio of 0.14 wt.% (Li/natural graphite). The mixed materials were added to ethanol and then ball-milled (150 rpm) for 20 h to ensure the formation of a homogeneous starting mixture. The slurry was dried at 85°C for 24 h. To eliminate organic components. The resulting powder was calcined in a furnace at 450°C for 5 h under air atmosphere.

Electrochemical characterization was performed by using a CR 2032 coin-cell type.

The cell consisted of a graphite electrode and a counter electrode (lithium metal) that were separated by a porous poly-ethylene film. The anode was prepared by spreading a mixture of 90 wt.% Li-doped natural graphite and 10 wt.% PVDF binder (KUREA, KF-1100) on to a copper foil current-collector. The graphite loading on the current-collector was typically 5.6 mg cm^{-2} . The electrolyte used in all experiments was 1 M LiPF_6 in ethylene carbonate and dimethyl carbonate (EC:DMC; vol. 1:2). The charge–discharge current density was 65 mA g^{-1} (0.2C-rate) with a cut-off voltage of 0.01–1.5 V at room temperature (30°C).

3. Results and discussion

X-ray diffraction patterns of samples of pristine graphite and Li ($x = \text{wt.}\%$)-doped natural graphite prepared by the ball-milling method are shown in Fig. 1(a) and (b), respectively. In the former, the peaks between 42° and 47° belong

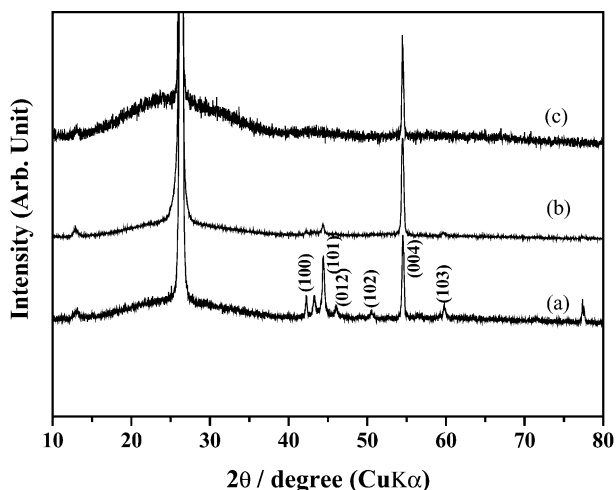


Fig. 1. XRD patterns of: (a) pristine natural graphite; (b) modified natural graphite prepared by calcination after ball-milling treatment without Li-doping; (c) Li 0.14 wt.%-doped natural graphite.

to the rhombohedra or hexagonal phase of natural graphite. The same peaks are also observed in the XRD profile for modified natural graphite prepared by calcination after ball-milling treatment in the ethanol for 20 h without Li-doping (Fig. 1(b)). The relative intensities are, however, greatly diminished. This indicates that the milling process reorientates the graphite crystals parallel to the basal plane and, at the same time, introduces stacking disorder [16]. The XRD profile of a sample of Li 0.14 wt.%-doped natural graphite prepared by calcination after ball-milling treatment is given in Fig. 1(c). The XRD profile of Li 0.14 wt.%-doped natural graphite is diffuse except for the (001) peaks. The XRD pattern suggests that Li treatment and subsequent ball-milling lead to the formation of very fine crystals, so-called ‘disordered’ graphite [17].

The cycling behaviour (specific discharge capacity versus cycle number) at the 0.2 rate of a pristine graphite electrode, a modified natural graphite prepared by calcination after ball-milling treatment without Li-doping and a Li ($x = 0.14\text{ wt.}\%$)-doped natural graphite electrode is shown in Fig. 2. The data clearly demonstrate the superior cycleability of the Li-doped graphite electrode, which provides a high discharge capacity of 358 mAh g^{-1} (i.e., close to theoretical value of 372 mAh g^{-1} based on LiC_6) and an excellent capacity retention of $\sim 99\%$ after 50 cycles. By comparison, the pristine natural graphite gradually lost its discharge capacity and exhibited a poor capacity retention of $<85\%$ after 50 cycles. It is worth noting that the irreversible capacity loss experienced by the Li-doped graphite electrode on the first charge–discharge process is only 7.4%, whereas the pristine graphite electrode and graphite electrode prepared by calcination after ball-milling treatment without Li-doping suffer losses of 13.2 and 11.1%, respectively. Moreover, the discharge capacity of the 0.14 wt.%-doped natural graphite electrode is 23% higher than that of pristine natural graphite at a

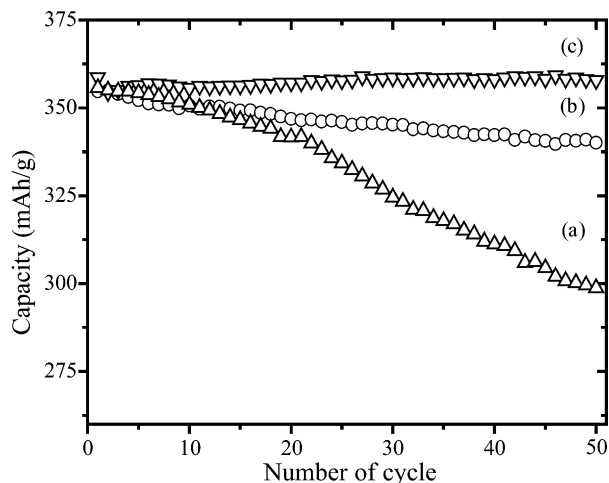


Fig. 2. Specific discharge capacity vs. number of cycles for: (a) pristine natural graphite; (b) modified natural graphite prepared by calcination after ball-milling treatment without Li-doping; (c) Li 0.14 wt.%-doped natural graphite.

high current density (3C-rate). Although other workers have proposed many surface modification methods, the Li-doping method presented here gives not only reduced irreversible capacity, but also superior cycling performance for greater periods. Natural graphite from a different source (Daebeck Co. Ltd., Korea) was also tested under the same conditions. This Li-doped graphite also displayed similar improvements in electrochemical properties (i.e., excellent capacity retention and a low irreversible capacity on the initial cycle), although the optimum level of doped lithium (Li 0.4 wt.-%-doping) was slightly different. Hence, it appears that the method of Li-doping proposed here can be applied regardless of the initial structural variations in the natural graphite.

The Li-doped natural graphite samples were further investigated to reveal the role of lithium in improving the cycle performance of natural graphite. Scanning electron microscopy (SEM) images of pristine graphite, graphite modified by calcination after ball-milling treatment without Li-doping, and Li 0.14 wt.-%-doped natural graphite are shown in Fig. 3. Since graphitic planes along the [002] direction are much more reactive compared with the basal planes, SEM measurements focused on the edges of the graphitic samples. Both untreated (Fig. 3(a)) and treated (Fig. 3(b)) samples prepared by calcination after ball-milling without Li-doping show sharp flat steps that extend straight along the edges. On the other hand, Li-doped graphite (Fig. 3(c)) exhibits rough edges with discontinuous steps and some of graphitic planes appeared to be curled up. These morphological changes suggest that lithium might have been incorporated along the edges of the natural graphite. Because X-ray diffraction (lattice parameter) did not indicate significant changes in the bulk structure, Li-intercalation appears to be restricted to near the edges of graphite.

X-ray photoelectron spectroscopy (XPS) spectra from Li-treated graphite prior to cycling are presented in Fig. 4. The measured binding energy (284.7 eV) and line shape of C 1s agree well with those of HOPG [18], which suggests that reaction of the graphite powder with Li during treatment is limited to localized areas. This is in agreement with the above conclusions drawn from SEM images. The O 1s spectrum has a relatively low intensity and its binding energy is ~ 531.5 eV, which nearly coincides with that of O 1s in Li_2O [19]. The binding energy of oxygen, together with its low concentration, suggests that surface modification is limited to the graphite edges and that Li exists in its oxide form at the graphite edges.

The electron diffraction pattern obtained by means of transmission electron microscopy (TEM) from one of the curled-up edges from the Li 0.14 wt.-%-doped sample is shown in Fig. 5. An extra row of spots (indicated by arrow) are observed (Fig. 5(a)). These do not exist in the graphite structure. These spots arise from stacking faults. When Li intercalates between two graphene layers, the stacking sequence for the graphitic sheets changes from the normal 'AB' registry to 'AA' [20]. This rotation of graphitic sheets into an 'AA' sequence creates the extra spots. Also observed from the

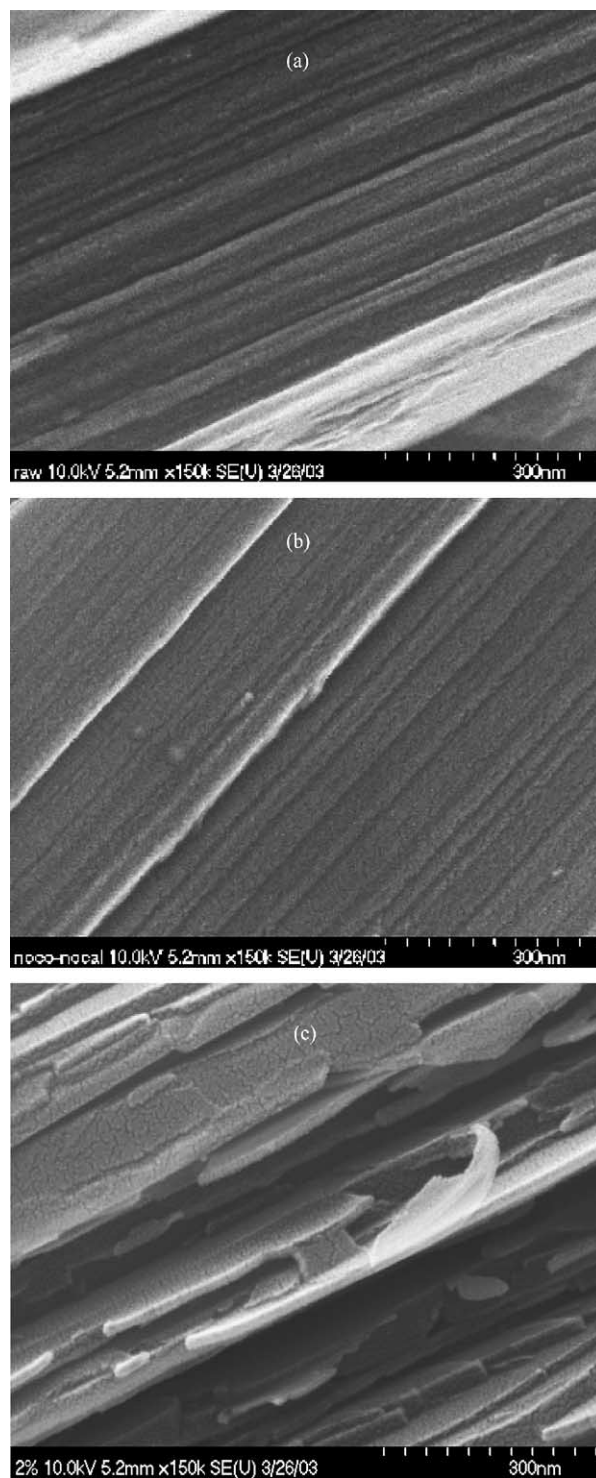


Fig. 3. SEM images of: (a) pristine natural graphite; (b) modified graphite prepared by calcination after ball-milling treatment without Li-doping; (c) Li 0.14 wt.-%-doped natural graphite.

diffraction pattern is streak normal to the C-axis, which provides further evidence for a thin platelet of structural faults normal to the C-axis [21]. Judging from the numerous satellite spots in the diffraction, the structure of Li-doped graphite is rather disordered around the edges due to the localized Li

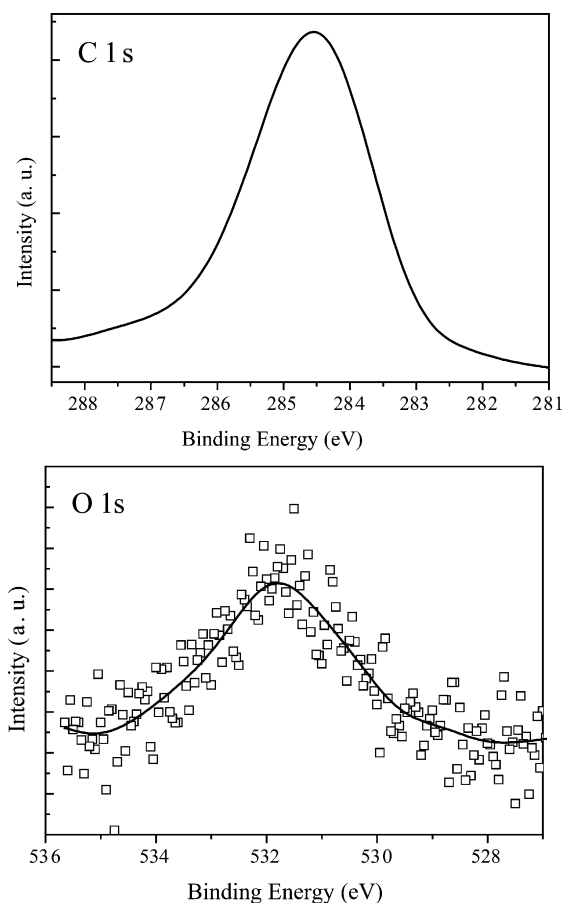


Fig. 4. C 1s and O 1s XPS spectra of Li 0.14 wt.%-doped natural graphite prior to cycling.

modification. A high-resolution TEM image of the sample in the same location is shown in Fig. 5(b). It clearly shows the disordered structure of the Li-doped graphite along the edges. Discontinuous (002) planes, stacking faults (indicated by the arrow) and contrast arising from the local stress in Fig. 3(b) provide direct evidence for localized intercalation along the edges of the natural graphite.

Localized Li-intercalation prior to cycling greatly improves the structural and chemical stability of the material. It is believed that LiO_x intercalated at the edges can reduce the electrolyte breakdown by passivating the highly reactive sites along the edge planes. This minimizes the formation of interfacial layers that block Li-intercalation and deintercalation. In addition, LiO_x located between adjacent graphitic planes can retard migration of large solvated Li-ions formed by the electrolyte solvent through the edge planes. Since the solvated Li-ions are unstable and irreversible in Li-intercalation, reduced intercalation of these large solvated Li-ions will help to preserve the structure of natural graphite anode.

When the surface of the basal plane in another part of the sample was observed with TEM, an amorphous layer with a thickness of about 50 Å was found. The amorphous layer appears to have formed on the surface of the material during calcination. The amorphous surface layer would reduce

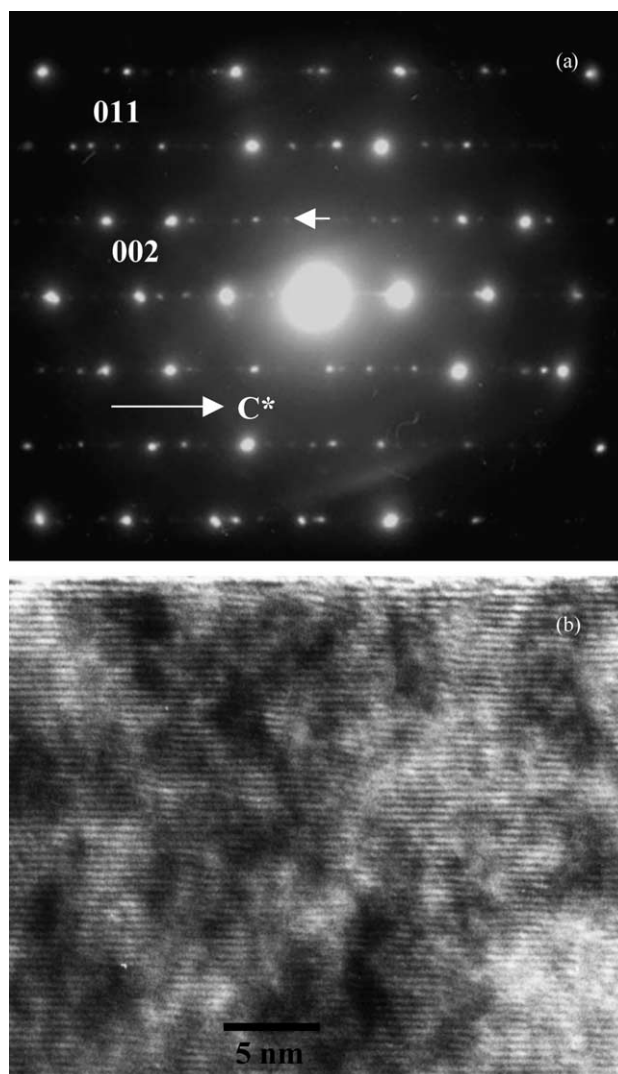


Fig. 5. (a) Electron diffraction pattern of 001 zone and (b) HRTEM image of (002) fringes from Li 0.14 wt.%-doped natural graphite.

active surface sites that may provide reaction sites for Li and therefore, would subsequently lead to capacity loss. In fact, limited improvement of electrochemical performance has been previously reported by coating the natural graphite with amorphous carbon. In conclusion, doping the natural graphite with Li prior to cycling, significantly enhances the cycling performance of the material. Conclusive evidence is found for localized LiO_x intercalation along the edges of the natural graphite and intercalated LiO_x appears to stabilize the graphite structure during electrochemical cycling.

4. Conclusion

The irreversible capacity loss of natural graphite during the first lithium intercalation–deintercalation process can be decreased (~5%) by modification of the graphite through lithium-doping. Also, lithium-doped natural graphite exhibits

improved capacity retention, because Li-doping stabilizes the structure of graphite during cycling. The improved performance is attributed to the presence of LiO_x along the edges of the graphite structure that minimizes electrolyte breakdown at the anode surface and the migration of solvated Li-ions.

Acknowledgements

This research was supported by University IT Research Center Project.

References

- [1] M. Inaba, Z. Siroma, A. Funabiki, Z. Ogumi, *Langmuir* 12 (1996) 1534.
- [2] J.-S. Kim, W.-Y. Yoon, K.S. Yoo, G.-S. Park, C.W. Lee, Y. Murakami, D. Shindo, *J. Power Sources* 104 (2002) 175.
- [3] T. Osaka, T. Momma, Y. Matsumoto, Y. Uchida, *J. Electrochem. Soc.* 144 (1997) 1709.
- [4] P. Arora, R.E. White, M. Doyle, *J. Electrochem. Soc.* 145 (1998) 3647.
- [5] V. Idota, T. Kubota, A. Matsufuji, Y. Mackawa, T. Miyasaka, *Science* 276 (1997) 1395.
- [6] I.A. Courtney, J.R. Dahn, *J. Electrochem. Soc.* 144 (1997) 2045.
- [7] I.A. Courtney, W.R. Mckinnon, J.R. Dahn, *J. Electrochem. Soc.* 46 (1999) 59.
- [8] H.Y. Lee, S.M. Lee, *J. Power Sources* 112 (2002) 649.
- [9] J. Read, D. Foster, J. Wolfenstine, W. Behl, *J. Power Sources* 96 (2001) 277.
- [10] J.Y. Lee, R. Zhang, Z. Liu, *Electrochem. Solid State Lett.* 3 (2000) 167.
- [11] E. Peled, C. Menachem, D. Bar-Tow, A. Melman, *J. Electrochem. Soc.* 143 (1996) L4.
- [12] C. Menachem, E. Peled, L. Buretein, Y. Rosenberg, *J. Power Sources* 68 (1997) 277.
- [13] M. Yoshio, H. Wang, K. Fukuda, Y. Hara, Y. Adachi, *J. Electrochem. Soc.* 147 (2000) 1245.
- [14] M. Yoshio, H. Wang, *J. Power Sources* 93 (2001) 123.
- [15] J. Drofenif, M. Gaberscek, R. Dominko, M. Bele, S. Pejovnik, *J. Power Sources* 94 (2001) 97.
- [16] T.S. Ong, H. Yang, *Carbon* 38 (2000) 2077.
- [17] H. Wakayama, J. Mizuno, Y. Fukushima, K. Nagano, T. Fukunaga, U. Mizutani, *Carbon* 37 (1999) 947.
- [18] C.M. Lee, B.J. Mun Jr., P.N. Ross, *J. Electrochem. Soc.* 149 (2002) A1286.
- [19] NIST, XPS spectra database, http://srdata.nist.gov/xps/main_search_menu.htm.
- [20] J.R. Dahn, T. Zheng, Y. Liu, J.S. Xue, *Nature* 17 (1995) 590.
- [21] B. Fultz, J.M. Howe, *Transmission Electron Microscopy and Diffraction of Materials*, Springer-Berlag, Berlin, 2001.